Received: 24 November 2022 | Accepted: 27 December 2022

DOI: 10.1111/1759-7714.14794

ORIGINAL ARTICLE

WILEY

Circ_0043256 upregulates KLF2 expression by absorbing miR-1206 to suppress the tumorigenesis of lung cancer

Ying Zhou[1] | Hongliu Liu[2] | Rui Wang[2] | Mingtao Zhang[2]

[1]Department of Respiratory and Critical Care Medicine, Jingmen No.1 People's Hospital, Jingmen, China

[2]Department of Oncology, Jingmen No.1 People's Hospital, Jingmen, China

Correspondence
Mingtao Zhang, Department of Oncology, Jingmen No.1 People's Hospital, No. 6, 12th Street, Fengyuan Road, Duodao, Jingmen, Hubei, China.
Email: zhangmingtao198609@163.com

Abstract

Background: Circular RNAs (circRNAs) have been reported to play roles in lung cancer development. The purpose of this work was to explore the function and mechanism of circ_0043256 in lung cancer tumorigenesis.

Methods: Quantitative real-time polymerase chain reaction (qRT-PCR) and western blot were used for the detection of the levels of genes and proteins. Cell growth, angiogenesis ability, migration, and invasion were analyzed by using 5-ethynyl-2′-deoxyuridine (EdU) assay, flow cytometry, tube formation assay, transwell assay, and murine xenograft model, respectively. The target between miR-1206 and circ_0043256 or Krüppel-like factor 2 (KLF2) was verified by dual-luciferase reporter assay.

Results: Circ_0043256 was a stable circRNA, which was found to be decreased in lung cancer tissues and cells. Functionally, forced expression of circ_0043256 suppressed lung cancer cell growth, angiopoiesis, migration, and invasion. Mechanistically, circ_0043256 directly bound to miR-1206 and miR-1206 targeted KLF2, circ_0043256 could regulate KLF2 expression via absorbing miR-1206. Rescue assay showed that miR-1206 overexpression reversed the anticancer effects of circ_0043256 on lung cancer cells. Moreover, inhibition of miR-1206 could suppress the malignant phenotypes of lung cancer cells, which was attenuated by KLF2 knockdown. Pre-clinically, lentivirus-mediated circ_0043256 overexpression impeded lung cancer growth in nude mice.

Conclusion: Forced expression of circ_0043256 could impede the tumorigenesis of lung cancer via miR-1206/KLF2 axis, indicating a potential therapeutic approach for lung cancer.

KEYWORDS
Angiogenesis, circ_0043256, KLF2, lung cancer, miR-1206

INTRODUCTION

Globally, lung cancer is still one of the most fatal malignancies, accounting for the leading cause of cancer death.[1] The morbidity of lung cancer is higher; there are ~1.76 million deaths and 2.09 million new cases in 2018.[1,2] Although progress has been made in treatment, the prognosis of lung cancer shows an unsatisfactory 5-year survival rate (16%) in patients who are diagnosed at late stage and metastasis.[3] Therefore, an in-depth understanding on the carcinogenesis of lung cancer is necessary for developing novel and effective therapeutic strategy.

Circular RNAs (circRNAs) are a class of conserved RNA molecules that are resistant to the degradation by exonuclease.[4,5] CircRNAs are implicated in regulating various cellular crucial biological processes linked with carcinogenesis, differentiation, growth, apoptosis, and drug resistance.[6–8] Moreover, deregulated circRNAs have been identified in lung cancer, and some circRNAs have crucial regulatory roles in the tumorigenesis of lung cancer.[9] For example, circRNA-002178 was confirmed to act as an oncogene in lung adenocarcinoma to stimulate T-cell exhaustion by

Ying Zhou and Hongliu Liu contributed equally to this paper.

elevating programmed death-ligand 1 (PDL1) expression.[10] Zhang et al.[11] showed that highly expressed hsa_circRNA_101237 was linked to poor outcome in lung cancer patients and knockdown of hsa_circRNA_101237 repressed cancer cell proliferative, migratory and invasive abilities. Moreover, circ_0007385 was also confirmed to promote lung cancer growth and cisplatin resistance.[12] In addition, a decreased circ_0043256 was found in lung cancer.[13] However, the action of circ_0043256 in lung cancer carcinogenesis remains unclear.

Here, this study focused on exploring the role of circ_0043256 in lung cancer cell malignant phenotypes and growth. It has been proposed that circRNAs can exert their functions by acting as competitive endogenous RNAs (ceRNAs), namely, circRNAs sequester microRNAs (miRNAs) to modulate the target genes.[14,15] Furthermore, a ceRNA network was constructed to elucidate the potential mechanism of circ_0043256 in lung cancer tumorigenesis.

MATERIAL AND METHODS

Human samples

In total, 36 pairs of tumor tissues and adjacent para-tumor tissues were collected from lung cancer patients at Jingmen No.1 People's Hospital. All cases did not obtain preoperative therapy. All samples were stored at −80°C. Informed consent was collected from all patients. This study was approved by the Ethics Committee of Jingmen No.1 People's Hospital according to the Declaration of Helsinki.

Cell culture

Human lung cancer cells (PC9 and A549) and normal human bronchial epithelial cell (Beas-2B) were obtained from Procell and cultured in Dulbecco's modified Eagle medium (Procell) harboring 1% antibiotics (Invitrogen) and 10% fetal bovine serum (FBS) (Procell) with 5% CO_2 at 37°C.

Cell transfection

The pCD5-ciR/circ_0043256 overexpression plasmids (oe-circ_0043256), Krüppel-like factor 2 (KLF2) specific small interference RNA (si-KLF2), miR-1206 mimic or inhibitor were constructed by GenePharma with empty pCD5-ciR plasmids (vector), non-target siRNA (si-NC), miR-NC, or miR-NC inhibitor as the contrasts. Thereafter, transient transfection was conducted using Lipofectamine 2000 (Invitrogen).

The overexpression plasmids of circ_0043256 were subcloned into a lentiviral vector (GenePharma) to establish a Lenti-oe-circ_0043256. The puromycin (2–5 μg/mL) was applied to select stable expressing lentiviral particles, which were then transfected into A549 cells for in vivo assay.

Subcellular fractionation and quantitative real-time polymerase chain reaction

The PARIS kit (Life Technologies) was applied to determine the cytoplasmic and nuclear circ_0043256 as per the instruction. Total RNA was extracted by using TRIzol reagent (Invitrogen). Approximately 3 μg isolated RNAs were treated with mock without the enzyme or 5 U/μg RNase R at 37°C for 20 minutes to assess the stability of circ_0043256. The complementary DNA (cDNA) was synthesized by using the Prime Script RT Reagent Kit (Takara), followed by quantitative real-time polymerase chain reaction (qRT-PCR) analysis with SYBR Green kit (Takara). The relative fold changes were calculated by $2^{-\Delta\Delta Ct}$ method and GAPDH or U6 was used as the internal reference. The primers are presented in Table 1.

5-Ethynyl-2′-deoxyuridine assay

After transfection, PC9 and A549 cells were placed into a 96-well plate containing 50 μM 5-Ethynyl-2′-deoxyuridine (EdU) labeling solution (RiboBio) and incubated for 3 hours. Following reacting with click reaction solution for 30 minutes, DAPI was used for cell nuclei staining. Finally, EdU-positive cells were detect to assess cell proliferation.

Colony formation assay

Following different transfection, PC9 and A549 cells (500/well) were added into a six-well plate with complete medium and incubated for 2 weeks. After being fixed by methanol and stained with 0.1% crystal violet (Sigma-Aldrich), visible colonies were imaged (100×) and counted using a microscope.

Flow cytometry

After transfection, PC9 and A549 cells were dyed with 10 μL Annexin V-FITC and 10 μL propiduim iodide (BD Biosciences) in the darkness for 15 minutes. Last, the FACSCanto II flow cytometer (BD Biosciences) was used to assay cell apoptosis.

Western blotting

Total protein was isolated by using RIPA buffer (Beyotime) containing protease inhibitors and the concentration of proteins was qualified by BCA detecting kit (Keygen). Next, protein electrophoresis membrane was transferred. Next, the

TABLE 1 Primers sequences used for PCR

Name		Primers for PCR (5'-3')
circ_0043256	Forward	TGTACATCGGCTGAGTGACG
	Reverse	GCCACCACCATGTTTCTATCC
KLF2	Forward	GTCCTTCTCCACTTTCGCCA
	Reverse	ACAGGATGAAGTCCAGCACG
miR-1206	Forward	GCCGAGTTCAAGTAATTCAGG
	Reverse	CTCAACTGGTGTCGTGGA
U6	Forward	CTCGCTTCGGCAGCACA
	Reverse	AACGCTTCACGAATTTGCGT
GAPDH	Forward	AAGGCTGTGGGCAAGGTCATC
	Reverse	GCGTCAAAGGTGGAGGAGTGG
ACACA	Forward	GAACCATCTCCCTTGGCCC
	Reverse	GCCCTCCTTCTCCTCCAGTA

circRNA

1. circ_0043256 circRNA Mature Sequence

AAACATGGTGGTGGCTTTGAAGGAGCTGTCTATTCGGGGTGACTTTCGAAC
TACAGTTGAATACCTGATCAAATTGTTAGAGACTGAAAGCTTTCAGATGAA
CAGAATTGATACTGGCTGGCTGGACAGACTGATAGCAGAAAAAGTACAGG
CTGAGCGACCTGACACCATGTTGGGGGTTGTGTGTGGTGCCCTCCACGTGG
CAGATGTGAGCCTGCGGAATAGCGTCTCTAACTTCCTTCACTCCTTAGAAA
GGGGTCAAGTCCTTCCTGCTCATACACTTCTGAATACAGTAGATGTTGAACT
TATCTATGAGGGAGTCAAGTATGTACTTAAGGTGACTCGACAGTCCCCCAA
CTCCTATGTGGTGATCATGAATGGCTCATGTGTAGAAGTAGATGTACATCGG
CTGAGTGACGGTGGACTGCTCTTGTCCTATGATGGCAGCAGTTATACTACGT
ATATGAAAGAGGAAGTGGATAG

2. circ_0043256 junction Sequence 3'end - 5'end of circRNA

CATGTGTAGAAGTAGATGTACATCGGCTGAGTGACGGTGGACTGCTCTTGTCCTATGATGGCA

GCAGTTATACTACGTATATGAAAGAGGAAGTGGATAG

AAACATGGTGGTGGCTTTGAAGGAGCTGTCTATTCGGGGTGACTTTCGAACTACAGTTGAATA

(Continues)

TABLE 1 (Continued)

CCTGATCAAATTGTTAGAGACTGAAAGCTTTCAGATG

3. NCBI 设计引物截图

https://www.ncbi.nlm.nih.gov/tools/primer-blast/primertool.cgi?ctg_time=1653472397&job_key=9_0os6SLqSOOHbMYvniXKsRjhhjpcJOF6A

Primer pair 1

	Sequence (5'->3')	Template strand	Length	Start	Stop	Tm
Forward primer	TGTACATCGGCTGAGTGACG	Plus	20	17	36	59.83
Reverse primer	GCCACCACCATGTTTCTATCC	Minus	21	115	95	58.98
Product length	99					

F: TGTACATCGGCTGAGTGACG
R: GCCACCACCATGTTTCTATCC

4. circRNA 引物验证

circ_0043256 junction Sequence 3'end - 5'end of circRNA

CATGTGTAGAAGTAGATGTACATCGGCTGAGTGACGGTGGACTGCTCTTGTCCTATGATGGCAGC
AGTTATACTACGTATATGAAAGAGGAAGTGGATAGAAACATGGTGGTGGCTTTGAAGGAGCTGTC
TATTCGGGGTGACTTTCGAACTACAGTTGAATACCTGATCAAATTGTTAGAGACTGAAAGCTTTC
AGATG

5、NCBI primer blast 特异性验证

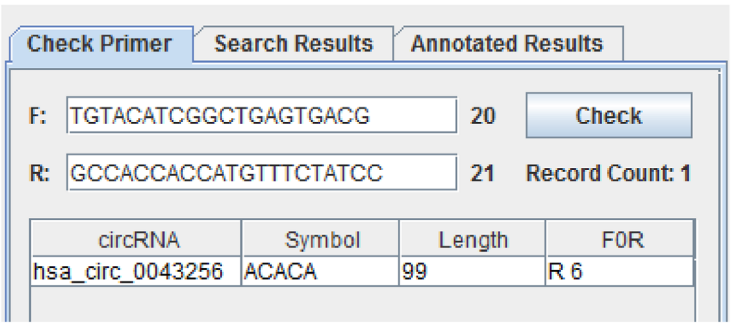

miRNA

1. 所用 miRNA mirbase 链接和成熟序列

>hsa-miR-1206 MIMAT0005870
UGUUCAUGUAGAUGUUUAAGC

(Continues)

TABLE 1 (Continued)

2. 把 U 替换为 T　TGTTCATGTAGATGTTTAAGC

3. 颈环通用序列　CTCAACTGGTGTCGTGGAGTCGGCAATTCAGTTGAGC

4. 上游引物（保护碱基+ miRNA 5 端的 13-16 个碱基）

GCCGAGTTCAAGTAATTCAGGAT

下游引物（茎环引物上的一段序列）

CTCAACTGGTGTCGTGGA

5. miRNA 验证

Accession	ID	Query start	Query end	Subject st
MIMAT0005870	hsa-miR-1206	7	21	1

Alignment of Query to mature miRNAs

Query: 7-21　hsa-miR-1206: 1-15　score: 75　evalue: 0.65

```
UserSeq        7  uguucauguagaugu  21
                  ||||||||||||||
hsa-miR-1206   1  uguucauguagaugu  15
```

6、NCBI 验证引物特异性

Primer pair 1

	Sequence (5'->3')	Length	Tm
Forward primer	GCCGAGTTCAAGTAATTCAGGAT	23	58.81
Reverse primer	CTCAACTGGTGTCGTGGA	18	56.51

靶基因

1. 基因转录本链接和截图

https://www.ncbi.nlm.nih.gov/nuccore/NM_016270.4

(Continues)

TABLE 1 (Continued)

Homo sapiens Kruppel like factor 2 (KLF2), mRNA

NCBI Reference Sequence: NM_016270.4

FASTA Graphics

Go to:

```
LOCUS       NM_016270               2820 bp    mRNA    linear   PRI 08-MAY-2022
DEFINITION  Homo sapiens Kruppel like factor 2 (KLF2), mRNA.
ACCESSION   NM_016270
VERSION     NM_016270.4
KEYWORDS    RefSeq; MANE Select.
SOURCE      Homo sapiens (human)
  ORGANISM  Homo sapiens
            Eukaryota; Metazoa; Chordata; Craniata; Vertebrata; Euteleostomi;
            Mammalia; Eutheria; Euarchontoglires; Primates; Haplorrhini;
```

2. NCBI primer blast 链接和截图(验证)

https://www.ncbi.nlm.nih.gov/tools/primer-blast/primertool.cgi?ctg_time=1653530780&job_key=dnyphmvaZnJBTGNJbilHexQyVkk5IU1UOA

Primer pair 1

	Sequence (5'->3')	Template strand	Length	Start	Stop	Tm
Forward primer	GTCCTTCTCCACTTTCGCCA	Plus	20	125	144	59.97
Reverse primer	ACAGGATGAAGTCCAGCACG	Minus	20	246	227	60.04
Product length	122					

Products on intended targets

>NM_016270.4 Homo sapiens Kruppel like factor 2 (KLF2), mRNA

```
product length = 122
Forward primer  1    GTCCTTCTCCACTTTCGCCA  20
Template        125  ....................  144

Reverse primer  1    ACAGGATGAAGTCCAGCACG  20
Template        246  ....................  227
```

F：GTCCTTCTCCACTTTCGCCA

R：ACAGGATGAAGTCCAGCACG

ACACA

2. 基因转录本链接和截图

https://www.ncbi.nlm.nih.gov/nuccore/NM_198834.3

(Continues)

TABLE 1 (Continued)

Homo sapiens acetyl-CoA carboxylase alpha (ACACA), transcript variant 1, mRNA

NCBI Reference Sequence: NM_198834.3

FASTA Graphics

Go to:

```
LOCUS       NM_198834              10013 bp    mRNA    linear   PRI 18-APR-2022
DEFINITION  Homo sapiens acetyl-CoA carboxylase alpha (ACACA), transcript
            variant 1, mRNA.
ACCESSION   NM_198834
VERSION     NM_198834.3
KEYWORDS    RefSeq; MANE Select.
SOURCE      Homo sapiens (human)
  ORGANISM  Homo sapiens
            Eukaryota; Metazoa; Chordata; Craniata; Vertebrata; Euteleostomi;
            Mammalia; Eutheria; Euarchontoglires; Primates; Haplorrhini;
```

3. NCBI primer blast 链接和截图(验证)

https://www.ncbi.nlm.nih.gov/tools/primer-blast/primertool.cgi?ctg_time=1653473260&job_key=5e86Fdf12139Y99m0gb7VKgd6maFDvF7hA&CheckStatus=Check

Primer pair 1

	Sequence (5'->3')	Template strand	Length	Start	Stop	Tm
Forward primer	GAACCATCTCCCTTGGCCC	Plus	19	655	673	60.08
Reverse primer	GCCCTCCTTCTCCTCCAGTA	Minus	20	789	770	60.03
Product length	135					

Products on intended targets

>NM_198834.3 Homo sapiens acetyl-CoA carboxylase alpha (ACACA), transcript variant 1, mRNA

```
product length = 135
Forward primer  1    GAACCATCTCCCTTGGCCC  19
Template        655  ...................  673

Reverse primer  1    GCCCTCCTTCTCCTCCAGTA  20
Template        789  ....................  770
```

F：GAACCATCTCCCTTGGCCC

R： GCCCTCCTTCTCCTCCAGTA

U6 通用引物

F：CTCGCTTCGGCAGCACA

R：AACGCTTCACGAATTTGCGT

(Continues)

TABLE 1 (Continued)

Primer pair 1

	Sequence (5'->3')	Length	Tm	GC%	Self complem
Forward primer	CTCGCTTCGGCAGCACA	17	60.42	64.71	5.00
Reverse primer	AACGCTTCACGAATTTGCGT	20	59.69	45.00	5.00

Products on target templates

>NR_104084.1 Homo sapiens RNA, U6 small nuclear 7 (RNU6-7), small nuclear RNA

```
product length = 94
Forward primer  1  CTCGCTTCGGCAGCACA  17
Template        4  .................  20

Reverse primer  1   AACGCTTCACGAATTTGCGT  20
Template        97  ..................  78
```

GAPDH

F 5'-AAGGCTGTGGGCAAGGTCATC-3',
R 5'-GCGTCAAAGGTGGAGGAGTGG-3'

Primer pair 1

	Sequence (5'->3')	Length	Tm	GC%	Self complementari
Forward primer	AAGGCTGTGGGCAAGGTCATC	21	62.96	57.14	3.00
Reverse primer	GCGTCAAAGGTGGAGGAGTGG	21	63.23	61.90	2.00

Products on target templates

>NM_001357943.2 Homo sapiens glyceraldehyde-3-phosphate dehydrogenase (GAPDH), transcript variant 7, mRNA

```
product length = 248
Forward primer  1    AAGGCTGTGGGCAAGGTCATC  21
Template        665  .....................  685

Reverse primer  1    GCGTCAAAGGTGGAGGAGTGG  21
Template        912  .....................  892
```

membrane was incubated with primary antibodies against Bax (ab32503, 1:2000, Abcam), Bcl-2 (ab692, 1:2000, Abcam), KLF2 (ab194486, 1:2000, Abcam), and β-actin (ab6276, 1:1000, Abcam) overnight at 4°C. After incubating with horseradish peroxidase (HRP)-conjugated secondary antibodies at 37°C for 2 hours, the chemiluminescent (ECL) detection reagent (Beyotime) was applied to assay the protein bands.

Tube formation assay

Each well of the 96-well plate was pre-coated with 50 μL Matrigel for 1 hour. The conditioned medium of transfected PC9 and A549 cells was collected. Human umbilical vein endothelial cells were starved for 24 hours and resuspended in 100 μL cell conditioned medium (4×10^5 cells/mL), and then seeded onto the Matrigel gel. Forty eight hours later, the number of tubes was detected by a microscope.

Transwell assay

Transwell chambers (8.0 μm pore size) (Corning) pre-coated with or without Matrigel (BD Biosciences) were used for cell invasion and migration detection. Transfected PC9 and A549 cells resuspended in serum-free medium were added into the upper chambers. Then, 500 μL of medium containing 10% FBS was filled into the lower chambers. Twenty-four hours later, migrated and invaded cells were fixed by 4% formalin and stained with crystal violet, and the number of cells were then counted using a microscope.

Dual-luciferase reporter assay

The wild-type (WT) fragments and the mutated (MUT) seed sequences of miR-1206 on circ_0043256 and KLF2 were inserted into the psiCHECK2 plasmids (Promega). Next, 200 ng recombinant psiCHECK2 plasmids and 50 nM miR-1206 or the controls were co-transfected into PC9 and A549 cells for 48 hours. The luciferase activity was assayed by a Dual-luciferase Reporter Assay System (Promega).

Xenograft models

The nude mice were divided into three groups (vector, oe-circ_0043256, or oe-circ_0043256 + miR-1206). A549 cells

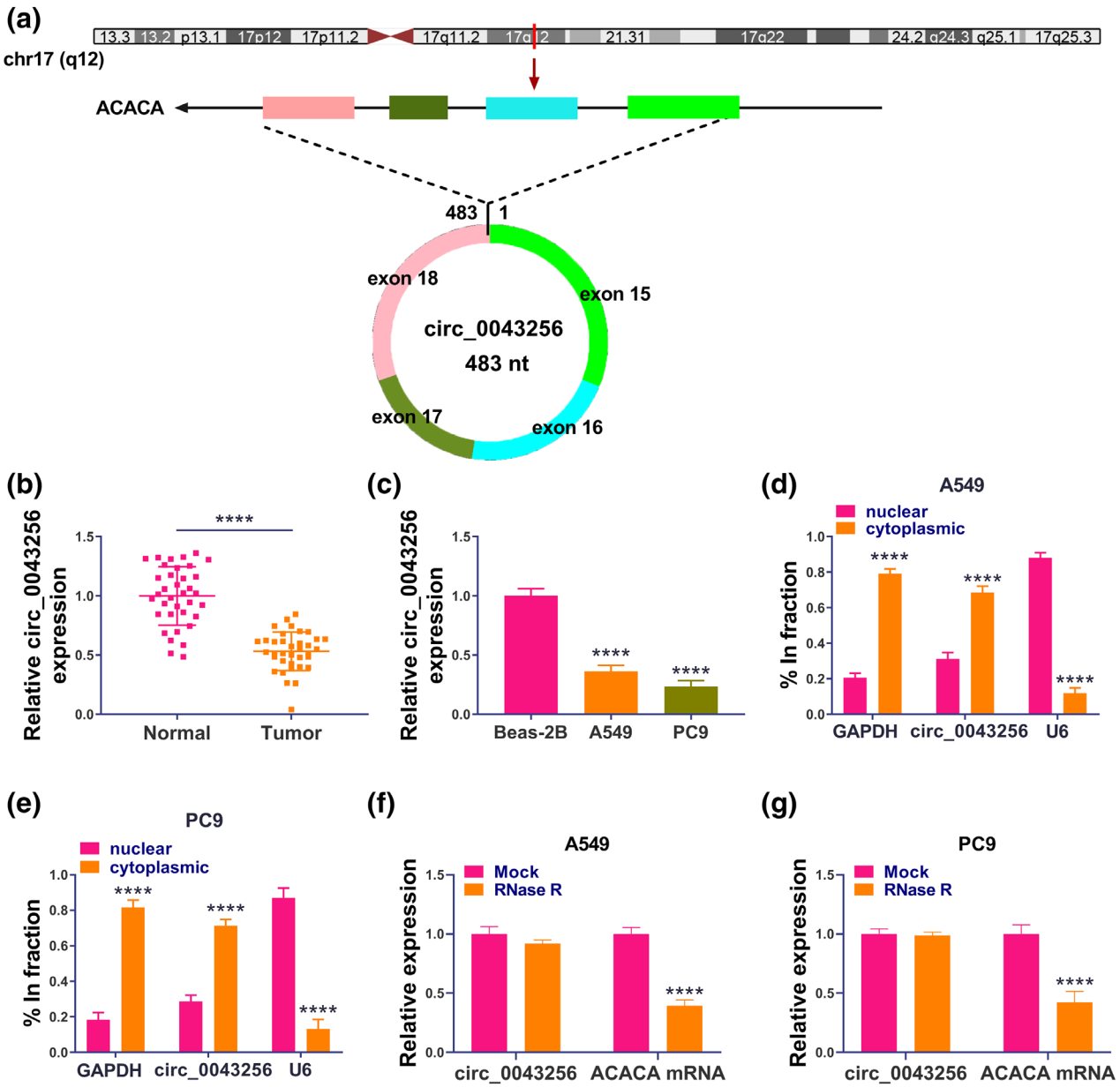

FIGURE 1 Circ_0043256 is decreased in lung cancer tissues and cells. (a) The genomic locus of circ_0043256 and the back-spliced junction of circ_0043256 were indicated. (b), (c) Detection of circ_0043256 expression in lung cancer tissues and normal tissues, as well as in lung cancer cell lines (PC9 and A549) and normal Bease-2B cells by quantitative real-time polymerase chain reaction (qRT-PCR). (d), (e) Nuclear-cytoplasmic fractionation assay for the distribution of circ_0043256 in PC9 and A549 cells. (f), (g) Stability analysis of circ_0043256 by RNase R treatment. ****$p < 0.0001$

infected with lentiviruses carrying oe-circ_0043256 or vector were subcutaneously vaccinated into the right back flank of blindly randomized nude mice (n = 5/group; 6 weeks). When the tumor grew to 100 mm^3, miR-1206 agonist was directly administered via intra-tumor injection into each mouse once a week for 4 weeks. The size of tumors was monitored every 7 days, and the volume was assessed as the formula: volume = length × $width^2$ × 0.5. Four weeks later, the tumors were excised, weighed, and divided either for molecule detection or fixed in formalin for immunohistochemistry (IHC) analysis as described previously.[16] The experiments abided the supervision of the Animal Care and Use Committee of Jingmen No. 1 People's Hospital.

Statistical assay

All experiments were repeated three times. Data are manifested as mean ± standard deviation (SD). The difference

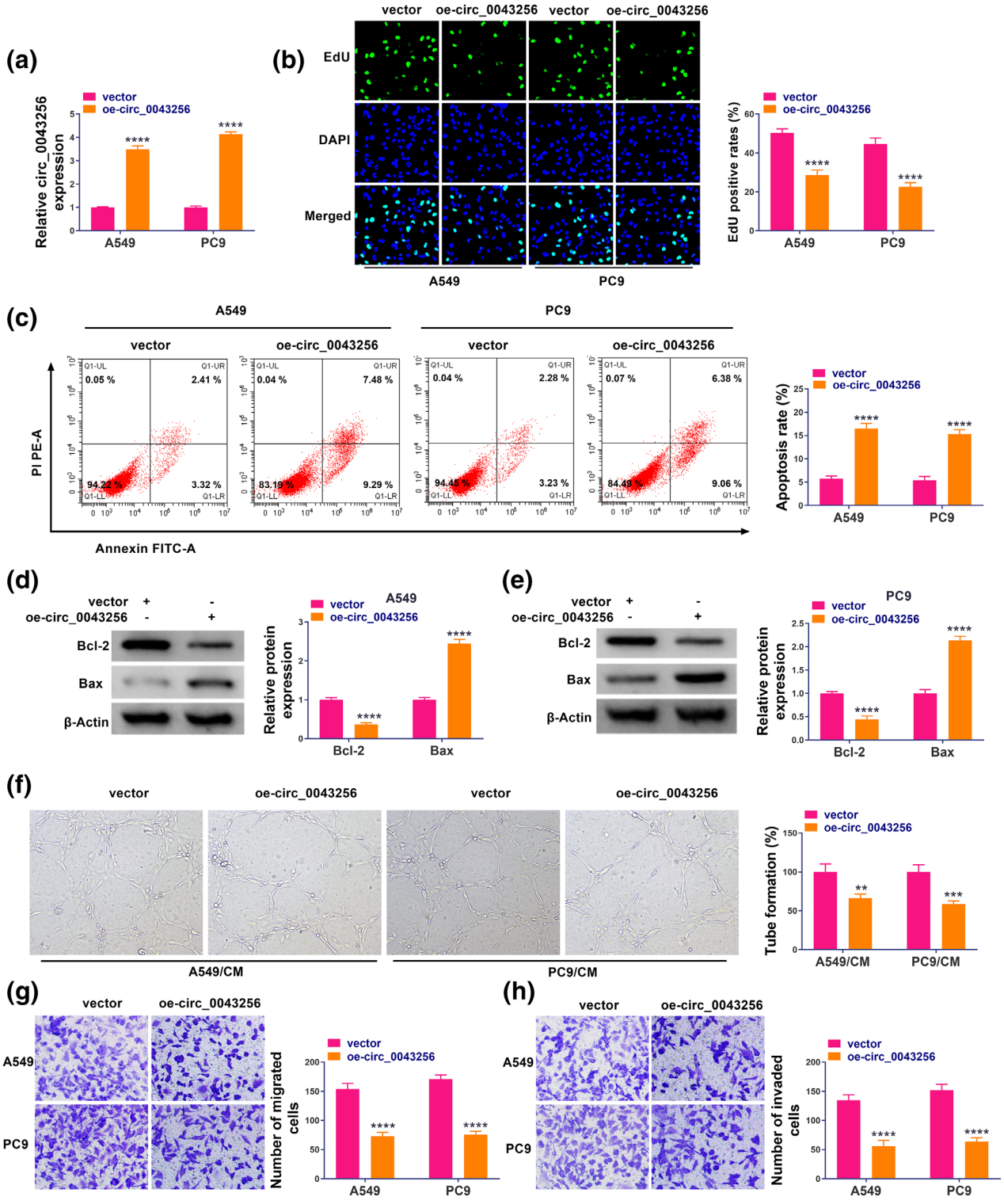

FIGURE 2 Overexpression of circ_0043256 suppresses lung cancer cell malignant phenotypes in vitro. (a)–(h) Oe-circ_0043256 or vector was constructed and transduced into A549 and PC9 cells. (a) Confirmation of the transfection efficiency by quantitative real-time polymerase chain reaction (qRT-PCR). (b) 5-Ethynyl-2′-deoxyuridine (EdU) assay for cell proliferation. (c) Flow cytometry for cell apoptosis. (d), (e) Western blotting analysis for the protein levels of Bax and Bcl-2. (f) Tube formation assay for cell tubule formation ability. (g), (h) Transwell assay for cell migration and invasion. ****$p < 0.0001$

was evaluated by the Student's *t*-test (two groups) and analysis of variance with Turkey test hoc post (multiple groups). $p < 0.05$ indicated significant differences.

RESULTS

Circ_0043256 is decreased in lung cancer tissues and cells

Circ_0043256 is produced by back-splicing of exon 15–18 of the ACACA gene, it is located at chr17: 35604934–35 609 962 and finally forms a circular transcript of 483 nt (Figure 1(a)). Circ_0043256 was found to be decreased in lung cancer tissues compared with the normal control (Figure 1(b)). Moreover, its expression was also lower in lung cancer cell lines (PC9 and A549) than those in normal Bease-2B cells (Figure 1(c)). The nuclear-cytoplasmic fractionation assay showed that circ_0043256 was mainly distributed in the cytoplasm of A549 and PC9 cells (Figure 1(d),(e)). In addition, it was observed that circ_0043256 was resistant to the degradation by RNase R in A549 and PC9, whereas RNase R treatment digested linear acetyl-CoA carboxylase α (ACACA) messenger RNA (mRNA) (Figure 1(f),(g)), implying that circ_0043256 was a stable circRNA.

Overexpression of circ_0043256 suppresses lung cancer cell malignant phenotypes in vitro

Next, the clinical value of circ_0043256 on lung cancer was investigated using in vitro assays. Circ_0043256 overexpression plasmids were constructed and transduced into A549 and PC9 cells. As expected, circ_0043256 expression was significantly elevated after oe-circ_0043256 transfection compared with vector transfection (Figure 2(a)). Functionally, forced expression of circ_0043256 suppressed the proliferation of A549 and PC9 cells, evidenced by decreased EdU-positive cells (Figure 2(b)). Moreover, colony formation assay also demonstrated that cell cloning capabilities of A549 and PC9 cells were suppressed after circ_0043256 overexpression (Figure S1(a)). Conversely, overexpression of circ_0043256 induced apoptosis in A549 and PC9 cells, which was accompanied with decreased Bcl-2 level and increased Bax level (Figure 2(c)–(e)). Moreover, circ_0043256 upregulation could impair tubule formation ability of A549 and PC9 cells (Figure 2(f)). In transwell assay, it

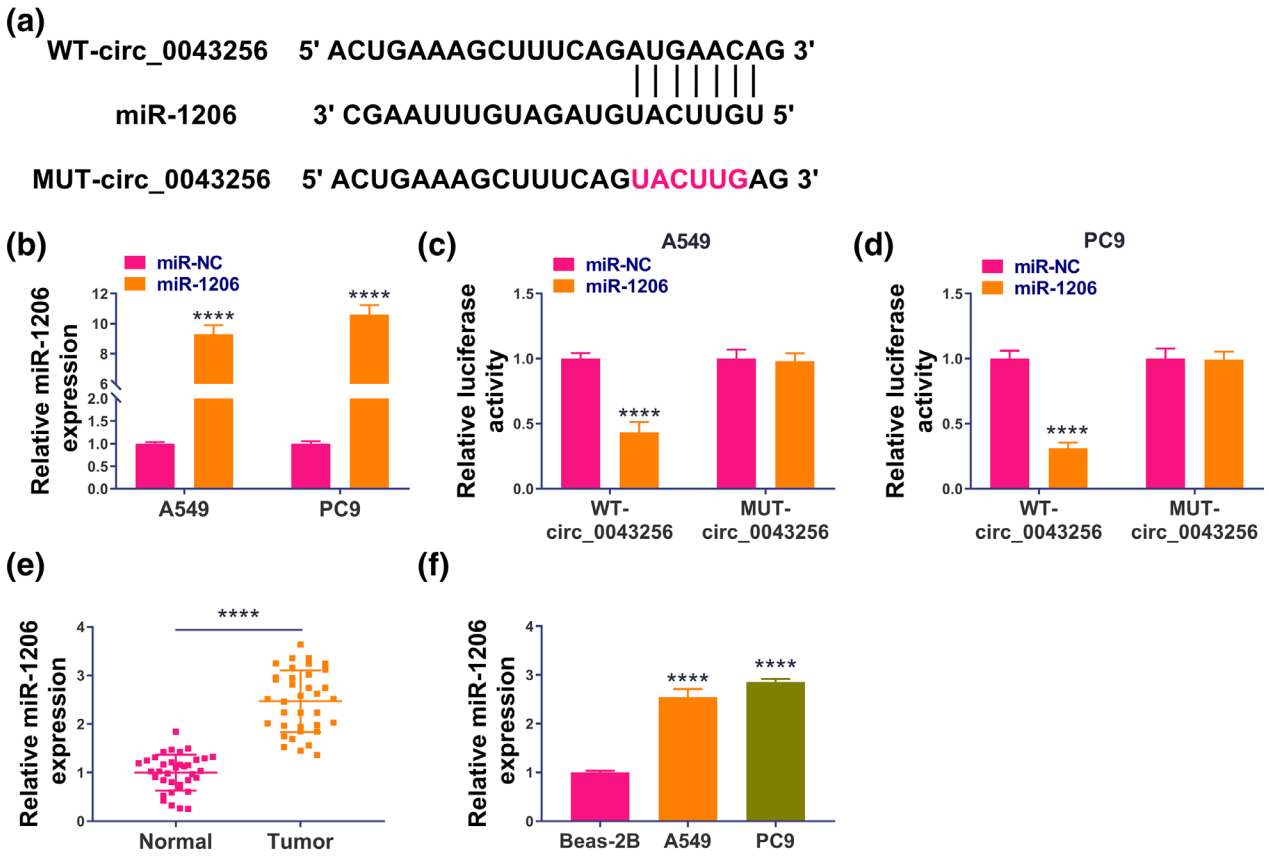

FIGURE 3 MiR-1206 is a target of circ_0043256. (a) The complementary sequences of miR-1206 on circ_0043256. (b) Confirmation of the transfection efficiency of the miR-1206 mimic or miR-NC by quantitative real-time polymerase chain reaction (qRT-PCR). (c), (d) Dual-luciferase reporter assay was used to verify the binding between miR-1206 and circ_0043256. (e), (f) Detection of miR-1206 expression in lung cancer tissues and normal tissues, as well as in lung cancer cell lines (PC9 and A549) and normal Bease-2B cells by qRT-PCR. ****$p < 0.0001$

was found that the migration and invasion abilities of A549 and PC9 cells were repressed after circ_0043256 upregulation (Figure 2(g),(h)). Taken together, circ_0043256 acted a tumor suppressor to inhibit lung cancer cell growth, angiopoiesis, migration, and invasion.

MiR-1206 is a target of circ_0043256

Given the cytoplasm distribution of circ_0043256, the downstream targets of circ_0043256 were investigated. According to the prediction of circinteractome, miR-1206 was found to have complementary sequences on circ_0043256 (Figure 3(a)). qRT-PCR showed that miR-1206 mimic could significantly elevate miR-1206 expression in A549 and PC9 cells (Figure 3 (b)). Next, dual-luciferase reporter assay was conducted. The results showed that miR-1206 mimic notably led to a decrease of the luciferase activity of WT-circ_0043256 vector, but bot the mutated one in A549 and PC9 cells (Figure 3(c),(d)). Moreover, miR-1206 expression was higher in lung cancer tissues and cell lines than those in normal controls (Figure 3(e), (f)). In all, circ_0043256 directly targeted miR-1206.

Overexpression of circ_0043256 suppresses malignant phenotypes mediated by miR-1206 in lung cancer cells

Next, we explored whether the anticancer effects of circ_0043256 was mediated by miR-1206. A549 and PC9 cells were transfected with oe-circ_0043256 alone or co-transfected with oe-circ_0043256 and miR-1206. qRT-PCR showed that oe-circ_0043256 transfection suppressed miR-1206 expression level in A549 and PC9 cells, which was

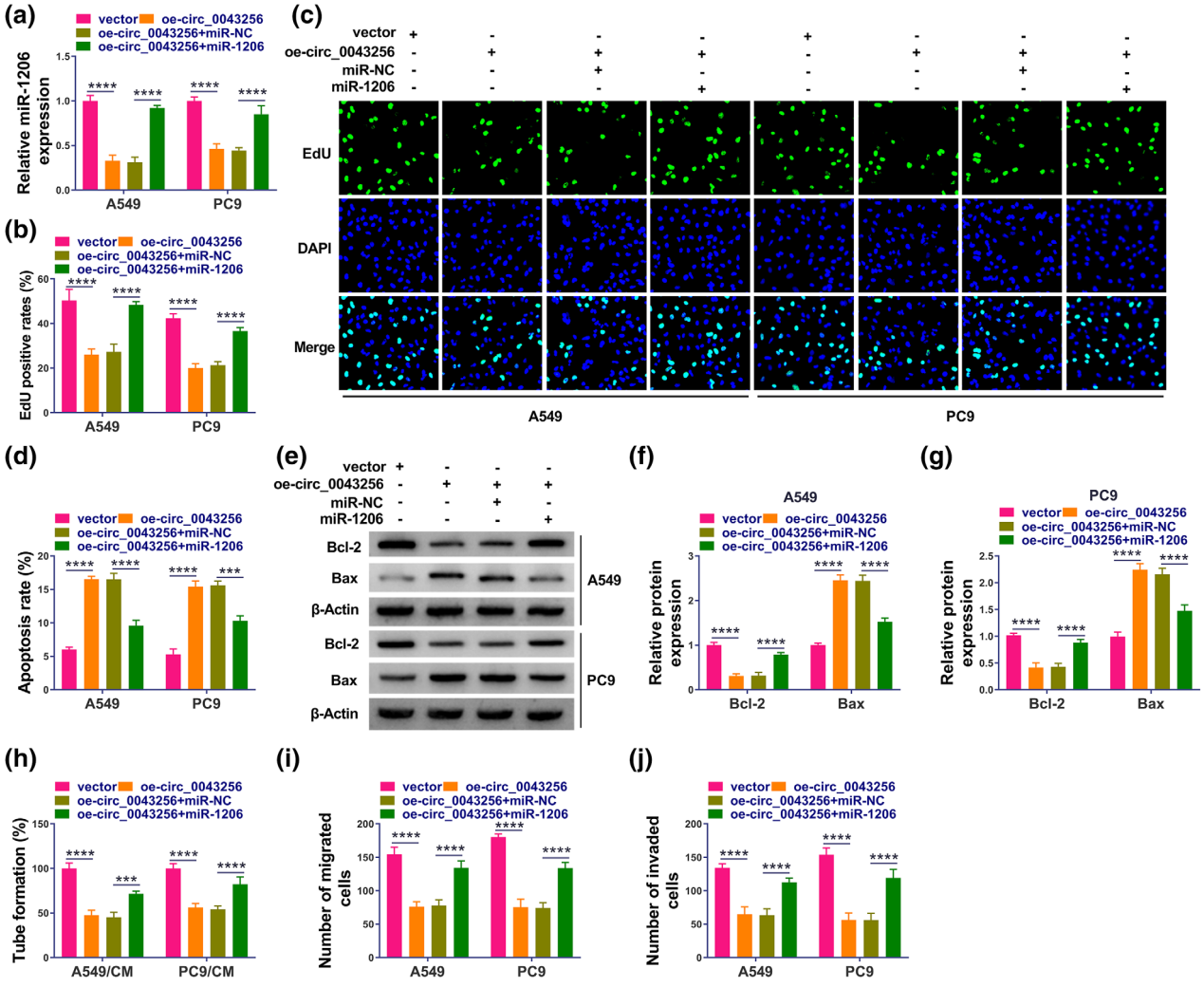

FIGURE 4 Overexpression of circ_0043256 suppresses malignant phenotypes mediated by miR-1206 in lung cancer cells. (a)–(j) A549 and PC9 cells were transfected with oe-circ_0043256 alone or co-transfected with oe-circ_0043256 and miR-1206. (a) Quantitative real-time polymerase chain reaction (qRT-PCR) for miR-1206 levels in cells. (b) (c) 5-Ethynyl-2′-deoxyuridine (EdU) assay for cell proliferation. (d) Flow cytometry for cell apoptosis. (e)–(g) Western blotting analysis for the protein levels of Bax and Bcl-2. (h) Tube formation assay for cell tubule formation ability. (i) and (j) Transwell assay for cell migration and invasion. $^{***}p < 0.001$, $^{****}p < 0.0001$

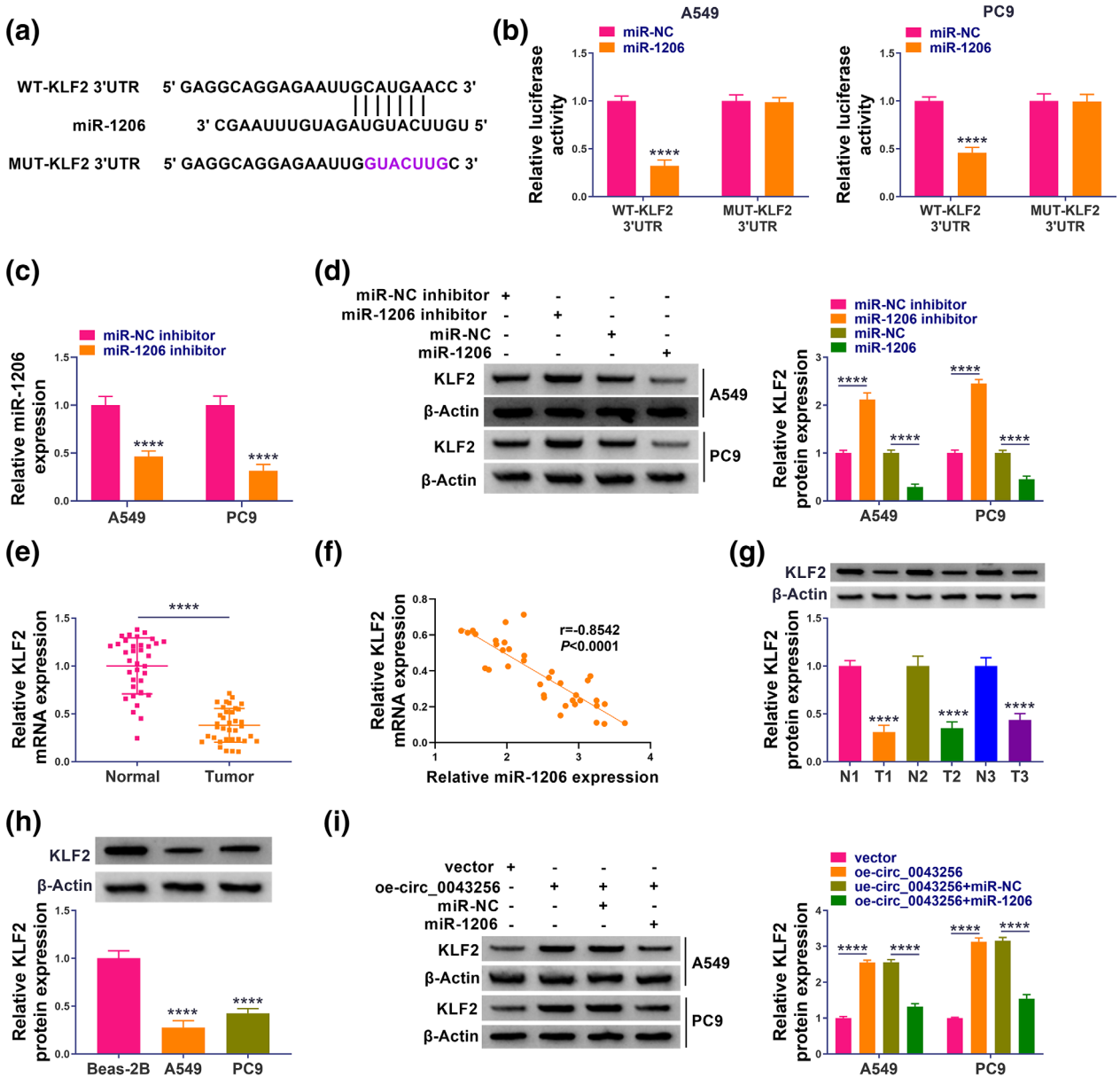

FIGURE 5 Krüppel-like factor 2 (KLF2) is a target of miR-1206, and circ_0043256 can regulate KLF2 by sponging miR-1206. (a) The binding site of miR-1206 on KLF2 3'UTR. (b) Dual-luciferase reporter assay was used to verify the binding between miR-1206 and KLF2. (c) Confirmation of the interference efficiency of miR-1206 inhibitor or miR-NC inhibitor by quantitative real-time polymerase chain reaction (qRT-PCR). (d) Western blot analysis of KLF2 expression in cells after miR-1206 increase or decrease. (e) Detection of KLF2 mRNA expression in lung cancer tissues and normal tissues by qRT-PCR. (f) The negative correlation between KLF2 mRNA expression and miR-1206 expression in cancer tissues. (g), (h) Detection of KLF2 protein expression in lung cancer tissues and normal tissues as well as in lung cancer cell lines (PC9 and A549) and normal Bease-2B cells by western blotting. (i) The effects of circ_0043256/miR-1206 axis on KLF2 expression. $^{****}p < 0.0001$

rescued by the introduction of miR-1206 (Figure 4(a)). Thereafter, it was found that miR-1206 up-regulation attenuated circ_0043256 overexpression-induced proliferation inhibition (Figure 4(b),(c) and Figure S1(b)) and apoptosis enhancement (Figure 4(d)–(g)). Moreover, the suppression of cell angiopoiesis, migration, and invasion abilities caused by circ_0043256 was also reversed by miR-1206 upregulation in A549 and PC9 cells (Figure 4(h)–(j)). These data confirmed that circ_0043256 affected lung cancer cell tumorigenesis via regulating miR-1206.

KLF2 is a target of miR-1206, and circ_0043256 can regulate KLF2 by sponging miR-1206

The targets of miR-1206 were also explored. Targetscan database predicted that miR-1206 had the binding site on KLF2 3'UTR (Figure 5(a)). The results of dual-luciferase reporter assay further exhibited that miR-1206 overexpression declined the luciferase activity of WT-KLF2 3'UTR vector, but bot affected the luciferase activity of MUT-KLF2 3'UTR in A549 and PC9 cells (Figure 5(b)). After

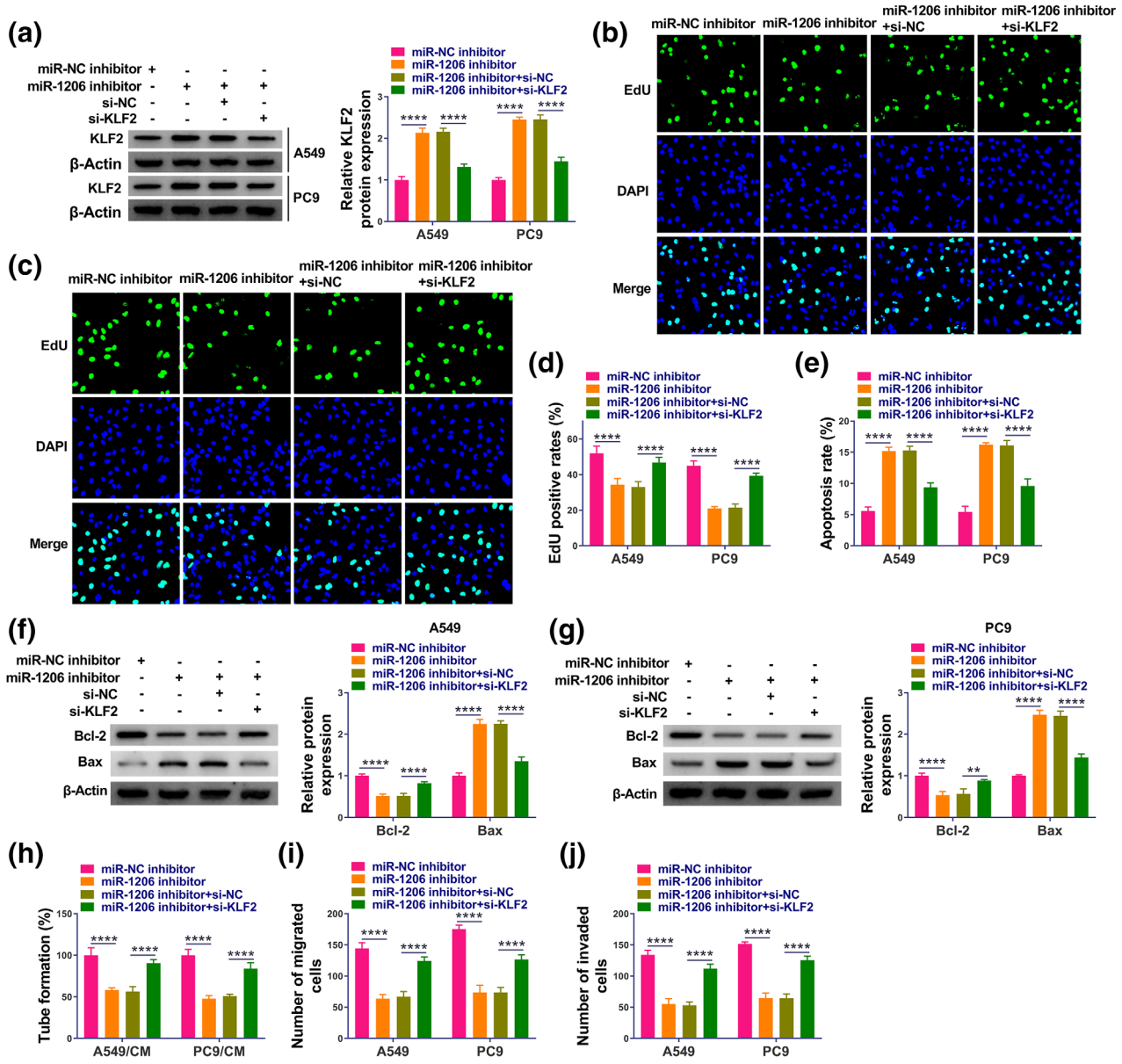

FIGURE 6 Knockdown of miR-1206 inhibits lung cancer cell malignant phenotypes by Krüppel-like factor 2 (KLF2). (a)–(j) A549 and PC9 cells were transfected with miR-1206 inhibitor alone or co-transfected with miR-1206 inhibitor and si-KLF2. (a) Western blotting for KLF2 levels in cells. (b)–(d) 5-Ethynyl-2′-deoxyuridine (EdU) assay for cell proliferation. (e) Flow cytometry for cell apoptosis. (f), (g) Western blotting analysis for the protein levels of Bax and Bcl-2. (h) Tube formation assay for cell tubule formation ability. (i), (j) Transwell assay for cell migration and invasion. $^{**}p < 0.01$, $^{****}p < 0.0001$

confirming the knockdown efficiency of miR-1206 inhibitor (Figure 5(c)), it was confirmed that KLF2 expression level was decreased by miR-1206 mimic and increased by miR-1206 inhibitor (Figure 5(d)). The mRNA content of KLF2 was found to be decreased in lung cancer tissues and was negatively correlated with miR-1206 expression in cancer tissues (Figure 5(e),(f)). Western blotting analysis also showed the decreased KLF2 protein level in lung cancer tissues (Figure 5(g)) and cell lines (Figure 5(h)). Interestingly, we also showed that oe-circ_0043256 introduction was accompanied with increased KLF2, which was subsequently reduced in response to miR-1206 mimic in A549 and PC9 cells (Figure 5(i)). Collectively, KLF2 was a target of miR-1206, and circ_0043256/miR-1206/KLF2 formed an axis.

Knockdown of miR-1206 inhibits lung cancer cell malignant phenotypes by KLF2

To evaluate the functions of miR-1206/KLF2 axis on lung cancer cell malignant phenotypes. The rescue experiments were performed. A549 and PC9 cells were transfected with miR-1206 inhibitor alone or co-transfected with miR-1206 inhibitor and KLF2 siRNA (si-KLF2). The western blotting

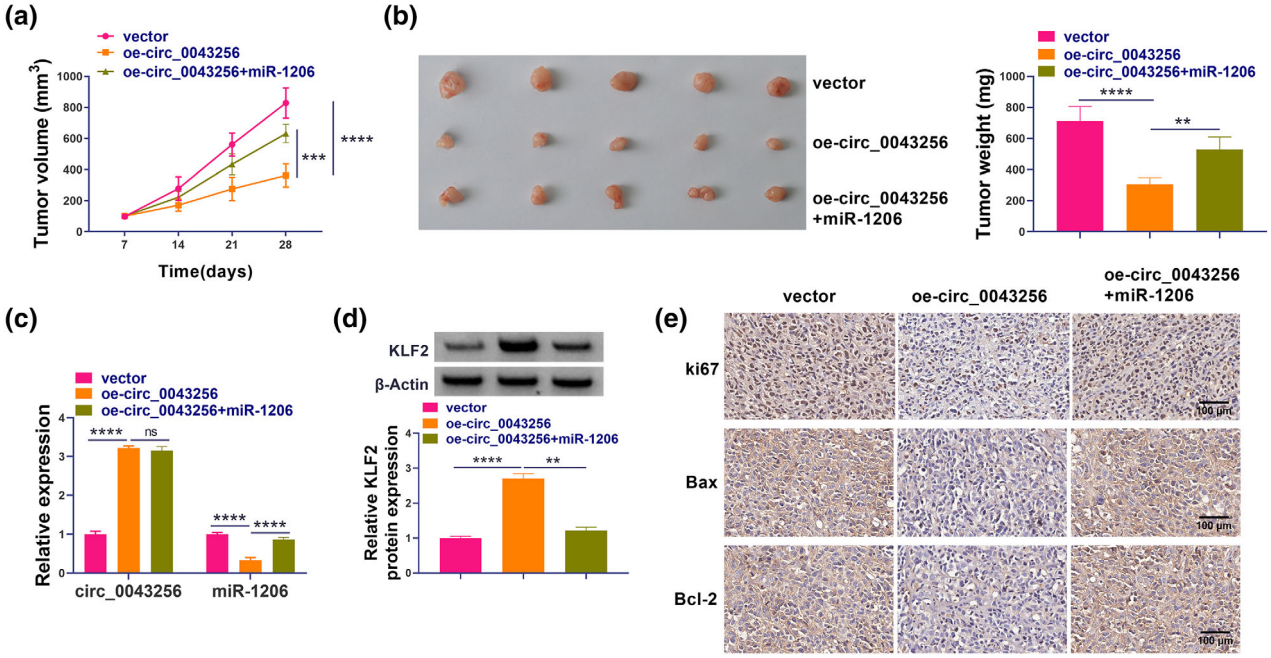

FIGURE 7 Overexpression of circ_0043256 suppresses lung cancer growth in vivo. (a), (b) In vivo growth curve (a), the representative images and tumor weight at the end points (b) of xenografts formed by subcutaneous injection. (c), (d) The levels of circ_0043256, miR-1206 and Krüppel-like factor 2 (KLF2) in xenografts were detected by using quantitative real-time polymerase chain reaction (qRT-PCR) or western blotting. (e) The quantification and representative images of immunohistochemistry staining revealing the expression of ki67, Bax, and Bcl-2 in subcutaneous xenografts. ****$p < 0.0001$

displayed that si-KLF2 introduction reversed miR-1206 inhibitor-induced elevation of KLF2 level in A549 and PC9 cells (Figure 6(a)). Functionally, we demonstrated that miR-1206 inhibitor could suppress cell proliferation (Figure 6(b)–(d) and Figure S1(c)) and stimulate apoptosis (Figure 6(e)–(g)) in A549 and PC9 cells, whereas these effects were reversed after KLF2 knockdown (Figure 6(b)–(g)). In addition, the angiopoiesis, migration, and invasion abilities of A549 and PC9 cells were markedly suppressed by miR-1206 inhibitor, which were then abolished by KLF2 silencing (Figure 6(h)–(j)). Altogether, miR-1206/KLF2 axis was engaged in regulating the tumorigenesis of lung cancer.

Overexpression of circ_0043256 suppresses lung cancer growth in vivo

Subsequently, we explored whether circ_0043256 affected the growth of lung cancer in vivo. Consistent with the results of in vitro experiments, overexpression of circ_0043256 hindered the growth of lung cancer in nude mice, reflected by the smaller tumor size and lighter tumor weigh in xenografts of oe-circ_0043256 group (Figure 7(a),(b)). Furthermore, compared with the oe-circ_0043256 group, the oe-circ_0043256 group + miR-1206 group showed bigger tumor size and heavier tumor weigh in xenografts (Figure 7(a),(b)). Moreover, the expression levels of circ_0043256 were higher in xenografts of oe-circ_0043256 group, whereas there was no change in the expression of circ_0043256 between oe-circ_0043256 group and oe-circ_0043256 group + miR-1206 group (Figure 7(c)). In addition, miR-1206 expression was decreased and KLF2 expression was increased in xenografts isolated from oe-circ_0043256 group, whereas these effects were attenuated after miR-1206 overexpression (Figure 7(c),(d)). Next, IHC analysis showed that the contents of ki67 and Bcl-2 were decreased, and Bax content was increased in xenografts with circ_0043256 overexpression, whereas oe-circ_0043256 group + miR-1206 group showed the opposite trend on their expression (Figure 7(e)). In all, circ_0043256 could suppress lung cancer growth in vivo.

DISCUSSION

Currently, more and more proofs have revealed that circRNAs are functional molecules that can modulate cancer progression by involving in various cellular activities. For instance, Chen et al.[17] showed that circRNA_0000285 silencing could repress the migration and growth abilities of cervical cancer in vitro and in nude mice. High has_circ_104348 predicted poor prognosis in hepatocellular carcinoma (HCC), and has_circ_104348 deficiency negatively regulated the malignant phenotypes of HCC cells.[18] In addition, Yuan et al. showed that circRNA_102231 promoted gastric cancer cell invasion and proliferation both in vitro and in vivo. Therefore, targeting the deregulation of circRNAs may be a promising method for cancer prevention. In our work, a decreased circ_0043256 was observed in lung cancer tissues and cells. Functionally, forced expression of

circ_0043256 restrained cancer cell proliferative, invasive, migratory, angiogenetic abilities and induced cell apoptosis in vitro. Pre-clinically, lentivirus-mediated circ_0043256 overexpression impeded lung cancer growth in nude mice, further indicting the anticancer potential of circ_0043256 in lung cancer.

This study verified the cytoplasmic distribution of circ_0043256 in lung cancer cells. Furthermore, the circRNA-miRNA-mRNA regulatory network has been identified to play crucial roles in the pathology of lung cancer.[19,20] Therefore, the potential miRNAs/mRNA axis underlying circ_0043256 was then explored. We confirmed that circ_0043256/miR-1206/KLF2 formed an axis in lung cancer cells. MiRNAs have been confirmed to be implicated in the modulation of the pathogenesis of human diseases, including the cancer.[21–23] MiR-1206 is a functional miRNA. It was found that could be used as the biomarker for ischemia reperfusion diagnosis.[24] MiR-1206 variant was confirmed to be related to methotrexate-induced oral mucositis in childhood acute lymphoblastic leukemia.[25] In cancer, Yu et al.[26] showed that circ_0092367 suppressed epithelial-mesenchymal transition process and gemcitabine resistance via miR-1206 in pancreatic cancer. Moreover, miR-1206 overexpression could reverse the anticancer effects of circ_0129047 or BMPR2 on lung adenocarcinoma.[27] KLF2 belongs to the Krüppel-like factor family transcription factors, which has been revealed to exert anticancer action in many types of cancers by impeding cancer cell malignant phenotypes.[28–30] In lung cancer, KLF2 expression was found to be decreased; restoration of KLF2 inhibited lung cancer cell proliferation.[31] In addition, KLF2 re-expression disturbed the proliferation of lung cancer cells by disappearing energy metabolism through glutaminase inhibition.[32] In our study, we also observed an increase of miR-1206 and a decrease of KLF2 in lung cancer tissues and cells. Moreover, miR-1206 promoted cancer cell proliferative, invasive, migratory, angiogenetic abilities, which were reversed by KLF2. Additionally, miR-1206 overexpression overturned the anticancer action of circ_0043256.

In all, we first confirmed that circ_0043256 acted as a tumor suppressor to restrain lung cancer growth and tumorigenesis by miR-1206/KLF2 axis, providing the molecular theoretical basis for subsequent clinical treatment of lung cancer.

AUTHOR CONTRIBUTION

Ying Zhou conceived and designed the study, and drafted the first draft of the manuscript. All experiments were completed by all authors. Hongliu Liu, Rui Wang, Mingtao Zhang analyzed and collated the results. All authors reviewed and critiqued the manuscript, and agreed to the final submission of the manuscript. All authors read and approved the final manuscript.

ACKNOWLEDGMENTS

None.

FUNDING INFORMATION

None.

CONFLICTS OF INTEREST

The authors declare they have no conflicts of interest.

ORCID

Mingtao Zhang https://orcid.org/0000-0003-4065-5274

REFERENCES

1. Bray F, Ferlay J, Soerjomataram I, Siegel RL, Torre LA, Jemal A. Global cancer statistics 2018: GLOBOCAN estimates of incidence and mortality worldwide for 36 cancers in 185 countries. CA Cancer J Clin. 2018;68:394–424.
2. Bade BC, Dela Cruz CS. Lung cancer 2020: epidemiology, etiology, and prevention. Clin Chest Med. 2020;41:1–24.
3. Mascaux C, Tomasini P, Greillier L, Barlesi F. Personalised medicine for nonsmall cell lung cancer. Eur Respir Rev. 2017;26:170066.
4. Yu J, Xu QG, Wang ZG, Yang Y, Zhang L, Ma JZ, et al. Circular RNA cSMARCA5 inhibits growth and metastasis in hepatocellular carcinoma. J Hepatol. 2018;68:1214–27.
5. Chen LL, Yang L. Regulation of circRNA biogenesis. RNA Biol. 2015;12:381–8.
6. Kristensen LS, Andersen MS, Stagsted LVW, Ebbesen KK, Hansen TB, Kjems J. The biogenesis, biology and characterization of circular RNAs. Nat Rev Genet. 2019;20:675–91.
7. Wu J, Qi X, Liu L, Hu X, Liu J, Yang J, et al. Emerging epigenetic regulation of circular RNAs in human cancer. Mol Ther Nucleic Acids. 2019;16:589–96.
8. Hua X, Sun Y, Chen J, Wu Y, Sha J, Han S, et al. Circular RNAs in drug resistant tumors. Biomed Pharmacother. 2019;118:109233.
9. Wang C, Tan S, Li J, Liu WR, Peng Y, Li W. CircRNAs in lung cancer - biogenesis, function and clinical implication. Cancer Lett. 2020;492:106–15.
10. Wang J, Zhao X, Wang Y, Ren FH, Sun DW, Yan YB, et al. circRNA-002178 act as a ceRNA to promote PDL1/PD1 expression in lung adenocarcinoma. Cell Death Dis. 2020;11:32.
11. Zhang ZY, Gao XH, Ma MY, Zhao CL, Zhang YL, Guo SS. CircRNA_101237 promotes NSCLC progression via the miRNA-490-3p/MAPK1 axis. Sci Rep. 2020;10:9024.
12. Ye Y, Zhao L, Li Q, Xi C, Li Y, Li Z. circ_0007385 served as competing endogenous RNA for miR-519d-3p to suppress malignant behaviors and cisplatin resistance of non-small cell lung cancer cells. Thorac Cancer. 2020;11:2196–208.
13. Li Y, Shi R, Zhu G, Chen C, Huang H, Gao M, et al. Construction of a circular RNA-microRNA-messenger RNA regulatory network of hsa_circ_0043256 in lung cancer by integrated analysis. Thorac Cancer. 2022;13:61–75.
14. Hansen TB, Jensen TI, Clausen BH, Bramsen JB, Finsen B, Damgaard CK, et al. Natural RNA circles function as efficient microRNA sponges. Nature. 2013;495:384–8.
15. Salmena L, Poliseno L, Tay Y, Kats L, Pandolfi PP. A ceRNA hypothesis: the Rosetta Stone of a hidden RNA language? Cell. 2011;146:353–8.
16. Zhou ZB, Huang GX, Fu Q, Han B, Lu JJ, Chen AM, et al. circRNA.33186 contributes to the pathogenesis of osteoarthritis by sponging miR-127-5p. Mol Ther. 2019;27:531–41.
17. Chen RX, Liu HL, Yang LL, Kang FH, Xin LP, Huang LR, et al. Circular RNA circRNA_0000285 promotes cervical cancer development by regulating FUS. Eur Rev Med Pharmacol Sci. 2019;23:8771–8.
18. Huang G, Liang M, Liu H, Huang J, Li P, Wang C, et al. CircRNA hsa_circRNA_104348 promotes hepatocellular carcinoma progression through modulating miR-187-3p/RTKN2 axis and activating Wnt/β-catenin pathway. Cell Death Dis. 2020;11:1065.

19. Fan Z, Bai Y, Zhang Q, Qian P. CircRNA circ_POLA2 promotes lung cancer cell stemness via regulating the miR-326/GNB1 axis. Environ Toxicol. 2020;35:1146–56.
20. Hong W, Xue M, Jiang J, Zhang Y, Gao X. Circular RNA circ-CPA4/let-7 miRNA/PD-L1 axis regulates cell growth, stemness, drug resistance and immune evasion in non-small cell lung cancer (NSCLC). J Exp Clin Cancer Res. 2020;39:149.
21. Bernardo BC, Ooi JY, Lin RC, McMullen JR. miRNA therapeutics: a new class of drugs with potential therapeutic applications in the heart. Future Med Chem. 2015;7:1771–92.
22. Mishra S, Yadav T, Rani V. Exploring miRNA based approaches in cancer diagnostics and therapeutics. Crit Rev Oncol Hematol. 2016; 98:12–23.
23. Rupaimoole R, Slack FJ. MicroRNA therapeutics: towards a new era for the management of cancer and other diseases. Nat Rev Drug Discov. 2017;16:203–22.
24. Abd El-Aziz A, El-Desouky MA, Shafei A, Elnakib M, Abdelmoniem AM. Influence of pentoxifylline on gene expression of PAG1/miR-1206/ SNHG14 in ischemic heart disease. Biochem Biophys Rep. 2021;25:100911.
25. Gutierrez-Camino A, Oosterom N, den Hoed MAH, Lopez-Lopez E, Martin-Guerrero I, Pluijm SMF, et al. The miR-1206 microRNA variant is associated with methotrexate-induced oral mucositis in pediatric acute lymphoblastic leukemia. Pharmacogenet Genomics. 2017;27:303–6.
26. Yu S, Wang M, Zhang H, Guo X, Qin R. Circ_0092367 inhibits EMT and gemcitabine resistance in pancreatic cancer via regulating the miR-1206/ESRP1 Axis. Genes (Basel). 2021;12:1701.
27. Xue X, Chen Y. Circular RNA (circ)_0129047 upregulates bone morphogenetic protein receptor type 2 expression to inhibit lung adenocarcinoma progression by sponging microRNA (miR)-1206. Bioengineered. 2022;13:12067–87.
28. Li Y, Tu S, Zeng Y, Zhang C, Deng T, Luo W, et al. KLF2 inhibits TGF-β-mediated cancer cell motility in hepatocellular carcinoma. Acta Biochim Biophys Sin (Shanghai). 2020;52:485–94.
29. Lu Y, Qin H, Jiang B, Lu W, Hao J, Cao W, et al. KLF2 inhibits cancer cell migration and invasion by regulating ferroptosis through GPX4 in clear cell renal cell carcinoma. Cancer Lett. 2021;522:1–13.
30. Yuedi D, Houbao L, Pinxiang L, Hui W, Min T, Dexiang Z. KLF2 induces the senescence of pancreatic cancer cells by cooperating with FOXO4 to upregulate p21. Exp Cell Res. 2020;388:111784.
31. Jiang W, Xu X, Deng S, Luo J, Xu H, Wang C, et al. Methylation of kruppel-like factor 2 (KLF2) associates with its expression and non-small cell lung cancer progression. Am J Transl Res. 2017;9:2024–37.
32. Xiao S, Jin-Xiang Y, Long T, Xiu-Rong L, Hong G, Jie-Cheng Y, et al. Kruppel-like factor 2 disturb non-small cell lung cancer energy metabolism by inhibited glutamine consumption. J Pharm Pharmacol. 2020; 72:843–51.

SUPPORTING INFORMATION

Additional supporting information can be found online in the Supporting Information section at the end of this article.

How to cite this article: Zhou Y, Liu H, Wang R, Zhang M. Circ_0043256 upregulates KLF2 expression by absorbing miR-1206 to suppress the tumorigenesis of lung cancer. Thorac Cancer. 2023;14(7):683–99. https://doi.org/10.1111/1759-7714.14794